Surface characterization and catalytic activity of sulfate-, molybdate- and tungstate-promoted Al$_2$O$_3$–ZrO$_2$ solid acid catalysts

Benjaram M. Reddy[a,*], Pavani M. Sreekanth[a], Yusuke Yamada[b], Tetsuhiko Kobayashi[b]

[a] *Inorganic and Physical Chemistry Division, Indian Institute of Chemical Technology, Hyderabad-500007, India*
[b] *National Institute of Advanced Industrial Science and Technology (AIST), Special Division of Green Life Technology, 1-8-31 Midorigaoka, Ikeda, Osaka 563-8577, Japan*

Abstract

Alumina–zirconia mixed oxide-supported sulfate-, molybdate- and tungstate-promoted solid acid catalysts were synthesized and characterized by various techniques. The Al–Zr hydroxide gel was obtained by a co-precipitation method from their corresponding nitrate salts by hydrolysis with aqueous ammonia. To the Al–Zr-hydrous mixed oxide support, aqueous solutions of sulfuric acid, ammonium heptamolybdate and ammonium metatungstate were added and the mixtures were refluxed at 110 °C, followed by evaporation of the water, drying and calcination at 650–750 °C. The surface and bulk properties of the catalysts were examined by using X-ray diffraction, BET surface area, TGA/DTA, ammonia-TPD and XPS techniques. The XRD results reveal that Al$_2$O$_3$–ZrO$_2$ mixed oxide calcined at 650 °C is in amorphous or poorly crystalline state exhibiting broad diffraction lines due to tetragonal ZrO$_2$ phase. At 750 °C calcination, a better crystallization of the zirconia tetragonal phase is observed. The XRD results further indicate that incorporation of alumina into zirconia stabilizes the tetragonal phase. The TGA–DTA studies provide information that there are at least two types of sulfate species with different thermal stabilities in the case of SO$_4^{2-}$/Al$_2$O$_3$–ZrO$_2$ catalyst. The TPD study reveals that the SO$_4^{2-}$/Al$_2$O$_3$–ZrO$_2$ catalyst exhibits an ammonia desorption peak maximum at 600 °C indicating super-acidic nature of the catalyst. The XPS peak intensities and the corresponding binding energies indicate that sulfate ion interacts with the support more strongly than other promoters. All characterization results provide information that the impregnated sulfate ions show a relatively strong influence on the physicochemical properties of the Al$_2$O$_3$–ZrO$_2$ mixed oxide. The prepared catalysts were evaluated for acetylation of alcohols and amines with acetic anhydride in the liquid phase. In line with physicochemical characteristics, the SO$_4^{2-}$/Al$_2$O$_3$–ZrO$_2$ exhibits better product yields under very mild reaction conditions.

1. Introduction

Solid acid catalysts are finding numerous applications in many areas of the chemical industry. These are extremely useful in many large volume applications, especially in the petroleum industry for alkylation and isomerization reactions [1–4]. Isomerization of *n*-alkanes into their corresponding branched alkanes is an important reaction in the petroleum industry to produce high-quality (high octane number) gasoline. Many catalysts were reported in the literature including AlCl$_3$ with additives like SbCl$_3$ and HCl, chlorinated alumina, transition metal-exchanged zeolites, heteropoly acids and some bifunctional catalysts [5]. Most of these isomerization catalysts suffer from different drawbacks such as high working temperature, continuous supply of chlorine and a high hydrogen pressure.

In recent years, promoted zirconia catalysts have gained much attention for isomerization reactions due to their super-

* Corresponding author. Tel.: +91 40 2716 0123; fax: +91 40 2716 0921.
E-mail addresses: bmreddy@iict.res.in, mreddyb@yahoo.com (B.M. Reddy).

acidity, non-toxicity and a high activity at low temperatures [2,4]. Among various catalysts, the sulfated zirconia has attracted much attention after its first report by Hino and Arata in 1979 [6]. This catalyst was also reported to be active for various organic transformations such as alkylation, acetylation, esterification, benzylation and some other condensation reactions [7–9]. However, a major disadvantage associated with sulfated zirconia is its rapid deactivation at high temperatures and under reducing atmosphere owing to the formation of SO_x and H_2S. Many efforts can be found in the literature to improve the activity and stability of the sulfated zirconia catalyst, including promotion of the catalyst with transition metals like Fe, Mn, Cr and with noble metal Pt [10]. Recently, some authors reported that sulfated zirconia-based mixed oxides show more stability and enhanced acidity than the transition/noble metal-promoted sulfated zirconia catalysts alone [11–14]. Three types of mixed oxides, namely SiO_2–ZrO_2 [12], Al_2O_3–ZrO_2 [13] and TiO_2–ZrO_2 [14] were mainly investigated for the sulfation and subsequent catalytic applications. In the case of SiO_2–ZrO_2 mixed oxide, the sulfate ion selectively interacts with non-silica component of the mixed oxide, i.e., zirconia. Hence, the sulfated silica–zirconia mixed oxide can be considered as sulfated zirconia dispersed on silica [12]. However, in the case of alumina–zirconia, the sulfate ion was found to interact strongly with both the components. Gao et al. [15] reported that addition of small amounts of alumina to sulfated zirconia enhances activity and stability of the catalyst for isomerization of *n*-butane. They observed that the surface sulfate ion concentration increases significantly with alumina content. The promotional effect of alumina on the sulfated zirconia catalyst was also confirmed by many others [16]. Skrdla and Lindemann [17] observed that sulfated Al_2O_3–ZrO_2 catalyst is very active for dehydration of 2-butanol. Furuta [18] reported that platinum-promoted sulfated alumina–zirconia catalyst shows enhanced activity than the platinum-promoted sulfated zirconia for light naphtha isomerization. Hino and Arata [19] observed that tungsten-oxide-promoted zirconia is an active catalyst for alkane isomerization and its acidity is stronger than that of 100% sulfuric acid. Based on Hammett acidity indicators, they suggested that the acidity of this catalyst is close to 14 ($H_0 \leq -14$). Subsequently, many groups confirmed that the acidity and catalytic activity of this catalyst is comparable to that of sulfated zirconia [20]. Our recent studies revealed that molybdenum-oxide-promoted zirconia also exhibits strong solid acidity and excellent catalytic properties for various organic synthesis and transformation reactions in the liquid phase [21–24].

In view of the above reasons, we were interested to investigate the precise role of promoters on the acidity of Al_2O_3–ZrO_2 and its application to various organic synthesis and transformation reactions. In this study, an alumina–zirconia mixed oxide was prepared by a homogeneous co-precipitation method and impregnated with sulfate, molybdate and tungstate promoters. The prepared catalysts were characterized by different physicochemical techniques, namely XRD, TGA/DTA, BET surface area, NH_3-TPD and XPS, and were evaluated for acetylation of alcohols and amines in the liquid phase.

2. Experimental

2.1. Catalyst preparation

The Al_2O_3–ZrO_2 binary oxide (1:1 mole ratio based on oxides) was prepared by a homogeneous coprecipitation method. For this purpose, an aqueous solution containing the requisite quantities of $Zr(NO_3)_4 \cdot xH_2O$ (Fluka, AR grade) and $Al(NO_3)_3 \cdot xH_2O$ (Loba Chemie, GR grade) were prepared separately and mixed together (pH 2). This solution was hydrolyzed with dilute ammonium hydroxide with vigorous stirring until the pH of the solution reached to 8–9. At this pH, a white precipitate was formed and the precipitate was allowed to settle for 2 days. The resulting precipitate was filtered off and washed several times with deionized water and dried at 120 °C for 12 h. The powdered oven-dried hydrous alumina–zirconia was immersed in 1 M H_2SO_4 solution (30 ml) for 30 min to incorporate sulfate ions. The excess water was evaporated on a water bath and the resulting sample was oven-dried at 110 °C for 12 h, calcined at 650 or 750 °C for 5 h, and finally stored in dry nitrogen atmosphere. The molybdate- and tungstate-promoted Al_2O_3–ZrO_2 catalysts, containing 10 wt.% MoO_3 or WO_3, were prepared by a suspension impregnation method. To incorporate molybdenum oxide or tungsten oxide, the requisite quantities of ammonium heptamolybdate (Fluka, AR grade) or ammonium metatungstate (JT Baker, England, GR grade) were dissolved in excess water and the finely powdered oven-dried hydrous alumina–zirconia support was added to this solution; each mixture was refluxed at 110 °C for 2 h. The excess water was evaporated on a water bath with continuous stirring. The resulting sample was oven-dried at 110 °C for 12 h, calcined at 650 or 750 °C for 5 h in air atmosphere, and finally stored in dry nitrogen atmosphere.

2.2. Catalyst characterization

X-ray powder diffraction patterns have been recorded on a Siemens D-5000 instrument by using a Cu Kα radiation source and a scintillation counter detector. The XRD phases present in the samples were identified with the help of JCPDS data files. The specific surface areas of the samples were determined on a Micromeritics Gemini 2360 instrument by N_2 physisorption at liquid nitrogen temperature and by taking 0.162 nm^2 as the molecular area of one N_2 molecule. Before measurements, all the samples were dried in situ at 200 °C for 2 h under vacuum.

The TGA/DTA analysis was carried out on a Mettler Toledo TG-SDTA apparatus (Pt crucibles, Pt/Pt–Rh thermocouple) with the purge gas (nitrogen) flow rate of 30 ml min^{-1} and the heating rate of 10 °C min^{-1} from 25 to 1000 °C.

The temperature-programmed desorption (TPD) measurements were performed on an AutoChem 2910 instrument (Micromeritics, USA). A thermal conductivity detector was used for continuous monitoring of the desorbed ammonia and the areas under the peaks were integrated. Prior to TPD measurements, samples were pretreated at $200\,^\circ$C for 1 h in a flow of ultrapure helium gas ($50\,ml\,min^{-1}$). After pretreatment, the sample was saturated with 10% ultrapure anhydrous ammonia gas (balance He, $75\,ml\,min^{-1}$) at $80\,^\circ$C for 2 h and subsequently flushed with He ($60\,ml\,min^{-1}$) at $110\,^\circ$C for 1 h to remove the physisorbed ammonia. The heating rate for the TPD measurements, from 110 to $800\,^\circ$C, was $10\,^\circ$C min^{-1}.

The XPS measurements were made on a Shimadzu (ESCA 3400) spectrometer by using Mg Kα ($1253.6\,eV$) radiation as the excitation source. Charging of the catalyst samples was corrected by setting the binding energy of the adventitious carbon (C 1s) at $284.6\,eV$ [25,26]. The XPS analysis was done at room temperature and at pressures typically in the order of less than 10^{-6} Pa. Samples were outgassed in a vacuum oven overnight before XPS measurements.

2.3. Catalyst evaluation

In a typical reaction procedure, a mixture of 1:1.5 molar amounts of alcohol/amine and acetic anhydride along with the catalyst (0.1 g) were taken into a round-bottomed flask and refluxed for various times. After completion of the reaction, the catalyst was filtered off and the wet catalyst was used for recycling. The product was recovered from the filtrate. An aqueous $NaHCO_3$ solution was added to remove the excess acetic anhydride. A 20 ml of CH_2Cl_2 solution was also added to separate aqueous and organic layers. The organic layer was decanted into another flask by using separating funnel and concentrated. The NMR and mass spectrometry techniques were utilized along with their melting/boiling points for analyzing the products.

3. Results and discussion

The prepared catalysts were subjected to TGA/DTA analysis before calcination. All samples showed a major weight loss peak in the range 70–130$\,^\circ$C corresponding to the loss of physically adsorbed water in the pores and on the surface of the samples. In the case of SO_4^{2-}/Al_2O_3–ZrO_2 sample, two weight loss peaks were observed at 783 and 891$\,^\circ$C, respectively. These high-temperature weight loss peaks could be due to decomposition of surface sulfate species at higher temperatures. This observation gives an impression that there are at least two types of sulfate species present with different thermal stabilities. Also the shift in the weight loss peaks towards higher temperatures when compared to that of SO_4^{2-}/ZrO_2 sample indicates an increase in the thermal stability of the surface sulfate species in the case of alumina–zirconia mixed oxide sample. A similar phenomenon was reported by Hua et al. [27] in the case of sulfated alumina–zirconia catalyst. An
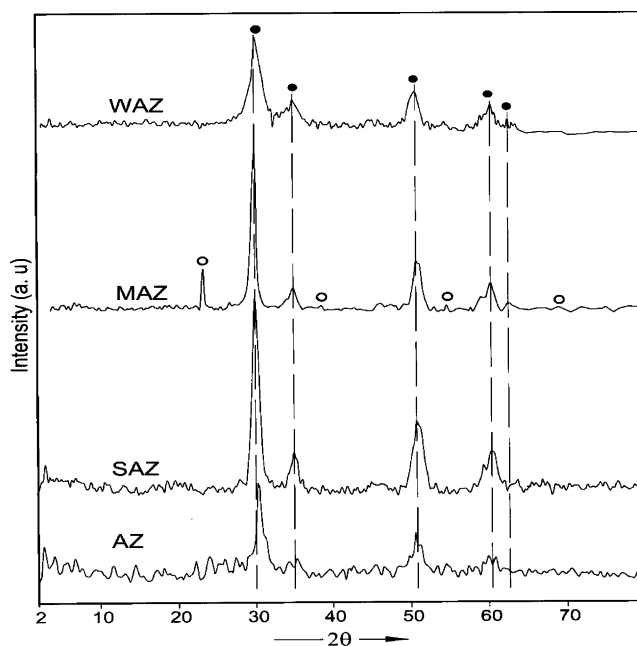

Fig. 1. X-ray powder diffraction patterns of Al_2O_3–ZrO_2 and promoted Al_2O_3–ZrO_2 samples calcined at $750\,^\circ$C: Lines due to (●) tetragonal ZrO_2 and (○) $Zr(MoO_4)_2$.

endothermic peak was also observed for SO_4^{2-}/Al_2O_3–ZrO_2 sample at higher temperatures due to phase transformation of alumina from gamma to alpha as reported in the literature [28]. No significant information was obtained from the TGA/DTA profiles of molybdenum oxide and tungsten oxide-promoted samples. Most importantly, the TGA/DTA results suggest that the optimum temperature for calcination of SO_4^{2-}/Al_2O_3–ZrO_2 samples is 600–650$\,^\circ$C where no loss of sulfate species could be observed.

The X-ray powder diffraction patterns of unpromoted and promoted Al_2O_3–ZrO_2 samples calcined at 750$\,^\circ$C are shown in Fig. 1. At 650$\,^\circ$C calcination temperature, all the samples are mainly in amorphous or poorly crystalline state. No independent lines due to crystalline alumina are observed indicating that alumina is homogeneously mixed with zirconia and in amorphous state. Only broad XRD lines due to tetragonal zirconia phase are observed. However, on increase of calcination temperature from 650 to 750$\,^\circ$C a better crystallization of tetragonal zirconia phase could be seen from Fig. 1. In the case of SO_4^{2-}/ZrO_2 samples, a mixture of tetragonal and monoclinic zirconia phases were mainly observed [24]. However, the XRD patterns of all promoted samples in the present study reveal only tetragonal phase, giving an impression that alumina acts as a structural stabilizer to zirconia. The addition of alumina to zirconia appears to retard the transformation of metastable tetragonal zirconia phase into more stable monoclinic phase. Stabilization of tetragonal zirconia by the addition of promoters such as La_2O_3, Y_2O_3, Yb_2O_3 and CaO is reported in the literature [29]. Zalewski et al. [30] reported that addition of alumina stabilizes the tetragonal zirconia phase by decreasing the crystallite size of

Table 1
BET surface area, total acidity and electron binding energies (eV) of pure and promoted Al_2O_3–ZrO_2 mixed oxide catalysts calcined at 650 °C

Sample	BET Surface area (m^2/g)	Total NH$_3$ desorbed (ml/g)	O 1s	Al 2p	Zr 3d$_{5/2}$	S 2p	Mo 3d$_{5/2}$	W 4f$_{7/2}$
Al_2O_3–ZrO_2	119	7.02	531.4	75.0	182.9	–	–	–
SO_4^{2-}/Al_2O_3–ZrO_2	33	15.03	532.4	75.1	183.1	169.8	–	–
Mo/Al_2O_3–ZrO_2	101	14.90	531.4	75.1	182.9	–	232.9	–
W/Al_2O_3–ZrO_2	114	19.39	531.6	75.2	182.9	–	–	36.3

zirconia. A further increase of calcination temperature from 750 to 850 °C revealed a high degree of crystallinity and a mixture of tetragonal and cubic zirconia phases.

The N$_2$ BET surface areas of various samples are shown in Table 1. As can be noted from this table, there is a slight decrease in the BET surface area of the Al_2O_3–ZrO_2 sample after impregnating with Mo- and W-oxides. However, in the case of sulfate ion-incorporated samples, the loss in the BET surface area is substantial. This could be due to the formation of non-porous Al and Zr sulfates at higher calcination temperatures. However, no XRD lines due to crystalline compounds of the same were observed. A similar phenomenon was also reported earlier in the case of sulfate ion-promoted alumina catalysts [4]. The small decrease observed in the case of Mo- and W-oxide-promoted catalysts could be due to penetration of these dispersed oxides into the pores of the Al–Zr binary oxide.

It is an established fact in the literature that ammonia is an excellent probe molecule for testing the acidic properties of solid catalysts. Its strong basicity and smaller molecular size allows detection of acidic sites located in the narrow pores of the solids. The ammonia-TPD profiles of pure and promoted Al_2O_3–ZrO_2 samples are shown in Fig. 2 and the corresponding total acidity results are presented in Table 1. As can be

noted from the TPD profiles, in all samples the acid sites are distributed in two temperature regions. The profiles of Mo/Al_2O_3–ZrO_2 and W/Al_2O_3–ZrO_2 are quite similar and show two desorption maxima. The second maximum at about 284 °C is sharper than the first one at ~200 °C. A similar two desorption processes are noted for SO_4^{2-}/Al_2O_3–ZrO_2 sample. The first desorption maximum observed at ~200 °C gradually decreases up to 500 °C. The second desorption process starts slowly above 520 °C and becomes rapid at ~600 °C as shown by a sharper maximum. This second desorption process or delay in NH$_3$ desorption indicates a stronger interaction of the acid sites with the adsorbed NH$_3$. Corma et al. [31] also reported the generation of a super-acidic peak at 550 °C in the NH$_3$-TPD of a sulfated zirconia catalyst calcined at 550 °C for 3 h. A similar ammonia desorption peak at 600 °C in the present study indicates the super-acidic nature of the SO_4^{2-}/Al_2O_3–ZrO_2 catalyst. The incorporation of Al_2O_3 into ZrO_2 and subsequent sulfation results in the shift of the temperature maximum from 550 to 600 °C. Desorption peaks with temperature maximum in the range 180–250, 280–330, 380–500 °C are normally attributed to NH$_3$ chemisorbed on weak, medium and strong acid sites, respectively [31]. Among all prepared catalysts, the SO_4^{2-}/Al_2O_3–ZrO_2 has the lowest amounts of weaker and moderate acid sites and the
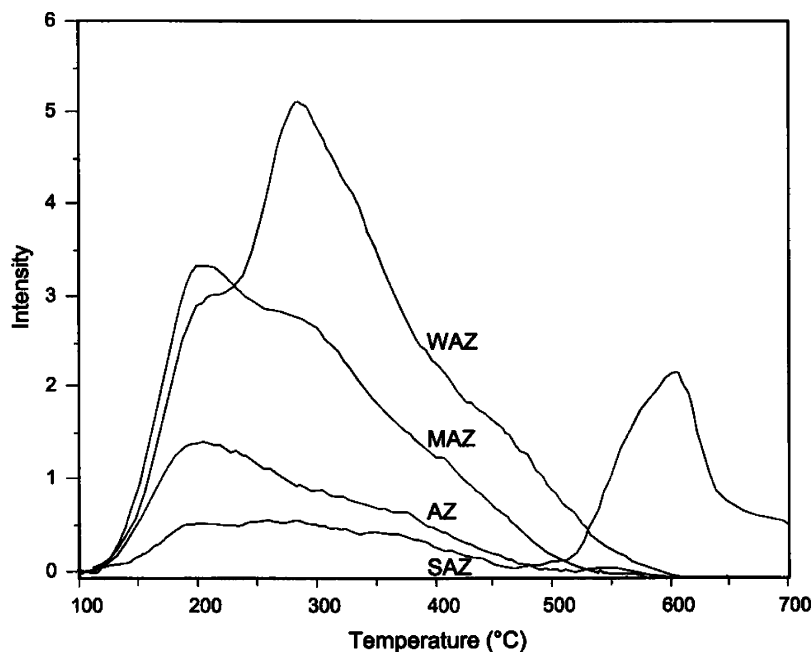

Fig. 2. The TPD of ammonia, after its adoption over various Al_2O_3–ZrO_2 samples at 80 °C and subsequent flushing at 110 °C.

highest concentration of stronger acid sites. When the promoters are incorporated into the Al_2O_3–ZrO_2, the distribution of acid strength normally changes. In the case of Mo- and W-oxide-incorporated catalysts, the concentration of medium strength acid sites increased drastically when compared to that of pure Al_2O_3–ZrO_2 support. In particular, the percentage of moderate strength acid sites on W/Al_2O_3–ZrO_2 is much higher than on the Mo/Al_2O_3–ZrO_2 sample. In general, in all cases the total number of acid sites is enhanced after incorporation of the promoters (Table 1).

X-ray photoelectron spectroscopy offers several advantages for the surface characterization of metal oxide catalysts. The relatively low kinetic energy (<1.5 keV) of the photoelectrons makes XPS inherently surface sensitive, which makes it ideal for characterizing ultra-thin oxide surfaces (1–10 nm). The unpromoted and promoted Al_2O_3–ZrO_2 samples calcined at 650 °C are investigated by XPS technique. The photoelectron peaks pertaining to O 1s, Zr 3d and Al 2p are shown in Figs. 3–5, respectively. The binding energies (E_b) of all the elements in these catalysts are shown in Table 1. Figs. 3–5 and Table 1 reveal that the photoelectron peaks of these samples are sensitive to the nature of the promoter atoms. As shown in Fig. 3, the O 1s profile is more broad due to overlapping contributions of oxygen atoms from alumina and zirconia in the case of Al_2O_3–ZrO_2 sample and similar contributions from sulfate, molybdate and tungstate in addition to the oxides of alumina and zirconia in the case of promoted catalysts. This figure shows that an extensive broadening of the O 1s peak of Al_2O_3–ZrO_2 sample occurred after impregnating with sulfate ions. The extent of peak broadening is less in the case of Mo- and W-oxide-promoted samples. The XPS peak intensity depends on both ion density and its chemical environment.
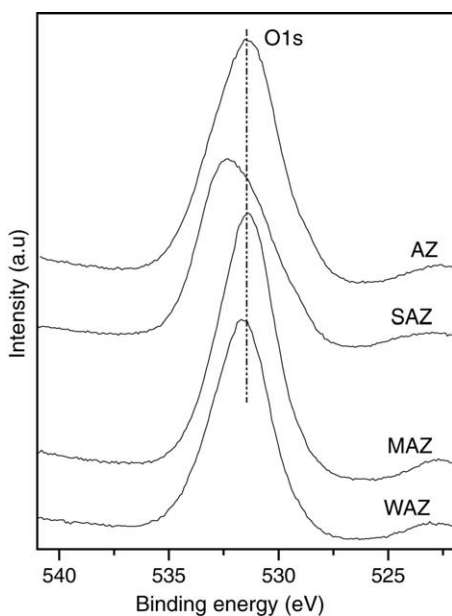

Fig. 4. The Zr 3d XPS spectra of Al_2O_3–ZrO_2 and promoted Al_2O_3–ZrO_2 samples calcined at 650 °C: (AZ) Al_2O_3–ZrO_2; (SAZ) SO_4^{2-}/Al_2O_3–ZrO_2; (MAZ) Mo/Al_2O_3–ZrO_2; (WAZ) W/Al_2O_3–ZrO_2.

The oxygen ion density in various samples is expected to be same. Therefore, the decrease or increase in the peak intensity can be attributed to different chemical environments. It is a known fact in the literature that broadening of the XPS peak depends on various factors including (i) the presence of more than one type of species with different chemical characteristics which cannot be discerned by ESCA and (ii) electron transfer between the promoter and the support [32]. The O 1s binding energies (Table 1) reveal that there is an increase in the binding energy in the case of SO_4^{2-}/Al_2O_3–ZrO_2 sample
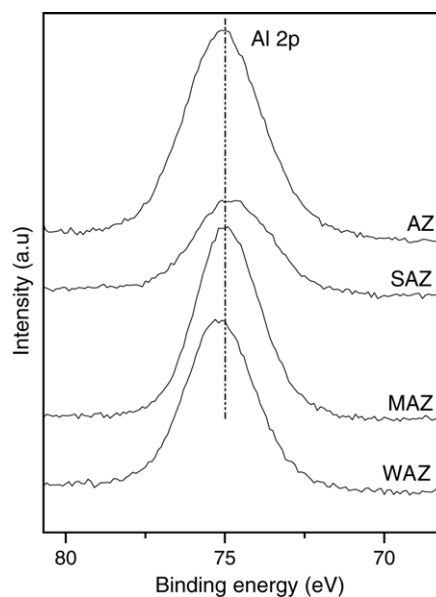

Fig. 3. The O 1s XPS spectra of Al_2O_3–ZrO_2 and promoted Al_2O_3–ZrO_2 samples calcined at 650 °C: (AZ) Al_2O_3–ZrO_2; (SAZ) SO_4^{2-}/Al_2O_3–ZrO_2; (MAZ) Mo/Al_2O_3–ZrO_2; (WAZ) W/Al_2O_3-ZrO_2.

Fig. 5. The Al 2p XPS spectra of Al_2O_3–ZrO_2 and promoted Al_2O_3–ZrO_2 samples calcined at 650 °C: (AZ) Al_2O_3–ZrO_2; (SAZ) SO_4^{2-}/Al_2O_3–ZrO_2; (MAZ) Mo/Al_2O_3–ZrO_2; (WAZ) W/Al_2O_3–ZrO_2.

when compared to that of other samples, due to the formation of the respective metal sulfates.

Fig. 4 shows the binding energy of the Zr 3d photoelectron peaks at 182.9 and 185.3 eV for Zr $3d_{5/2}$ and Zr $3d_{3/2}$ lines, respectively. The Zr 3d lines are reasonably well resolved with good intensity. Here too a significant broadening is noted in the case of sulfate-ion-promoted sample. A high intensity and better resolution of the peaks in the case of Mo- and W-promoted Al_2O_3–ZrO_2 catalysts could be due to better crystallization of the samples under the influence of promoters. A slight shift towards higher binding energy is noted in the case of sulfate-ion-promoted samples. The binding energy of the Zr $3d_{5/2}$ line in unpromoted ZrO_2 sample ranges between 182.2 and 182.5 eV [25,26]. An increase in the binding energy of the Zr 3d line in the case of Al_2O_3–ZrO_2 sample, in comparison to ZrO_2 alone, gives an impression that both the component oxides are mixed homogeneously to form a solid solution. Fig. 5 shows the binding energy of the Al 2p photoelectron peak in various samples at around 75.0 eV. Here too an extensive broadening of the Al 2p peak can be noted in the case of sulfate-ion-promoted sample. The Al 2p peak, in case of unpromoted Al_2O_3 samples, is normally observed at 74.7 eV [25,26]. A slight increase in the Al 2p binding energy can be noted for all Al_2O_3–ZrO_2 samples with respect to Al_2O_3. This observation indicates that alumina is strongly interacting with the zirconia and with the promoter atoms too.
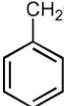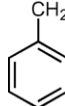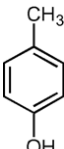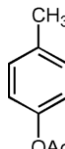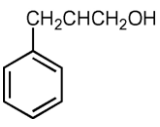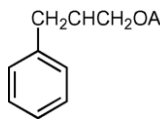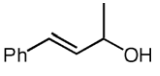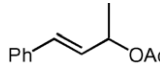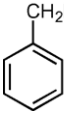
In the S 2p photoelectron spectrum of the SO_4^{2-}/Al_2O_3–ZrO_2 sample, two distinct 2p lines were observed, corresponding to the sulfates of individual metals. However, the spectrum was more complicated due to the overlapping contributions from Al- and Zr-sulfates as observed in the case of the O 1s line. The Mo $3d_{5/2}$ photoelectron peak of the Mo-oxide-promoted Al_2O_3–ZrO_2 sample was observed at 232.9 eV. Although, well-resolved Mo 3d lines were noted, they are very broad. The core level binding energy values indicate that the molybdenum is present in Mo(VI) oxidation state in the catalyst. As noted from XRD study, the molybdenum-oxide-promoted Al_2O_3–ZrO_2 sample contains a well-defined $Zr(MoO_4)_2$ compound, the precursor of which, the amorphous Zr–O–Mo, may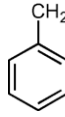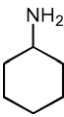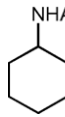 also be present [33–35]. The broadening of the Mo 3d line clearly indicates the presence of both. As presented in Table 1, the W $4f_{7/2}$ photoelectron peak of the W-oxide-promoted Al_2O_3–ZrO_2 catalyst was observed at 36.3 eV, which agrees well with the values reported in the literature for tungsten compounds [25,26]. Here too, the W 4f spectrum was not well resolved indicating a lack of well-defined W(VI) species. As pointed out earlier, there could be several reasons for the observed extensive broadening of the XPS peaks. These peaks indicate clearly that there are some undefined WO_x species that are present on the surface of the Al_2O_3–ZrO_2 support.

All the synthesized catalysts were evaluated for acylation of alcohols and amines with acetic anhydride in the liquid phase. The acylation reaction is a frequently used process in organic synthesis for derivatization and characterization of alcohols and also for further transformations. Acylation of alcohols and amines is an important method for preparing organic esters and amides, which are valuable intermediates for the production of fine chemicals. Traditionally, the acylation reactions are carried out by using activated acyl groups such as acid chlorides or acid anhydrides in the presence of basic catalysts such as 4-dimethylaminopyridine (DMAP), 4-pyrrolidinopyridine, trybutyl phosphene, Lewis acids like $AlCl_3$, $FeCl_3$, BF_3, indium(III) chloride and with conventional Brönsted acids such as sulfuric acid, polyphosphoric acid and hydrofluoric acid [36–38]. For conventional acylation reactions, Lewis acid catalysts and amine base catalysts are required in stoichiometric quantities. These catalysts form stable complexes with both the acylating agent and the product, thus preventing reuse of the catalysts. The solid acid-catalyzed acylation of alcohols and amines is a potential alternative to basic and nucleophilic catalysts. The introduction of solid acids facilitates the catalyst reuse through continuous operation of the reaction or by separating the catalyst from the reaction mixture by simple filtration. For this purpose, many solid acid catalysts were employed including montmorillonite K-10, silica-gel-supported $TaCl_5$, Nafion-H, yttria–zirconia, metal triflates and zeolites [39–43]. However, some of these protocols suffer from various drawbacks such as the use of excess acylating agent, stringent reaction conditions, use of halogenated solvents and some of the reagents employed are expensive (triflates). Although clays and zeolites showed improved reaction selectivity, activities of these catalysts are much lower than conventional homogeneous acids. Therefore, there is a need for efficient solid acid catalysts, which possess strong acid sites, water tolerant and reusable. In view of the significance of this reaction, the prepared catalysts were evaluated for acylation of alcohols and amines by using acetic anhydride as acylating agent. Results of the reaction carried out with sulfated alumina–zirconia are summarized in Table 2. In general, all the catalysts exhibited reactivity for this reaction under mild conditions. Among the four catalysts investigated in this study, the SO_4^{2-}/Al_2O_3–ZrO_2 showed better activity and selectivity followed by Mo/alumina–zirconia.

It is reported in the literature that the Al_2O_3–ZrO_2 shows increased acid site density than that of individual component oxides [44]. Mixed oxides often show enhanced acidity and thermal stability than their constituent single oxides. This is primarily due to the charge imbalance generated upon the minor component oxide by imposition of the bond matrix of the major component oxide [45]. In the case of 1:1 mole ratio mixed oxides enhanced acidity generates due to charge imbalance resulting from hetero-atom linkages. Various explanations can be found in the literature on the origin of stronger acidity in the case of sulfate-, molybdate- and tungstate-doped zirconia catalysts [4,20,46]. In particular, the surface acidity characterization of SO_4^{2-}/ZrO_2 shows that its surface contains very strong Brönsted acid sites as well as Lewis acid sites. The number and the strength of these sites largely vary with parameters such as sulfation method,

Table 2
Acetylation of alcohols and amines with $(Ac)_2O$ in the presence of $SO_4^{2-}/Al_2O_3–ZrO_2$

Entry	Alcohol/amine	Acetate	Time/yield
1	CH₂OH (benzyl alcohol)	CH₂OAc (benzyl acetate)	2/95
2	CH₃ ... OH (4-methylphenol)	CH₃ ... OAc	3/91
3	CH₂CHCH₂OH (phenyl)	CH₂CHCH₂OAc (phenyl)	2/89
4	Ph—CH=CH—CH(CH₃)—OH	Ph—CH=CH—CH(CH₃)—OAc	2/98
5	CH₂NH₂ (benzyl amine)	CH₂NHAc	1/92
6	NH₂ (cyclohexylamine)	NHAc	1/96

sulfur concentration, activation temperature and the nature of the precursor [7]. In the case of $Al_2O_3–ZrO_2$, the sulfate ion strongly interacts with both the components of the mixed oxide. Due to this, the surface sulfur concentration of this catalyst increases significantly.

The super-acidity of W/ZrO_2 and Mo/ZrO_2 catalysts was first observed by Arata and Hino [19,47]. They reported that solid superacids could be synthesized by supporting W- or Mo-oxides on ZrO_2 or TiO_2 under certain preparation conditions. Our recent investigations also revealed that the molybdate- or tungstate-promoted ZrO_2 catalysts exhibit strong solid acidity and interesting catalytic activity for various organic synthesis and transformation reactions in the liquid phase [21–23,48,49]. Although these catalysts are less active than sulfated zirconia, they show superior thermal stability in both oxidizing and reducing atmospheres. In W/ZrO_2 catalysts, WO_x clusters of intermediate size delocalize a net negative charge caused by a slight reduction of W^{6+} centers in reactant environments containing H_2 or hydrocarbons. This temporary charge imbalance leads to the formation of Brönsted acid sites on the zirconia support [50]. Generally, it is believed that tungsten oxide can exist on the zirconia surface in the form of polyoxotungstate clusters. Tungsten oxide is also known to form polytungstate layers on other oxides like Al_2O_3 and TiO_2, whereas on the

surface of silica it forms inactive WO_3 [51]. By considering the above facts, one can expect an enhanced acidity and stability for the tungsten-oxide-promoted $Al_2O_3–ZrO_2$ mixed oxide catalyst. Supported tungsten oxide catalysts have an advantage over heteropolytungstate catalysts. These catalysts retain their structural integrity even at high temperatures, whereas heteropolytungstates decompose to form bulk WO_3 at higher temperatures. Excellent review articles can be found in the literature on tungsten-oxide-based solid acid catalysts [50,52]. In conformity with this argument, some authors reported a high activity for tungsten-oxide-promoted alumina–zirconia catalysts for various reactions. Nagata et al. [53] reported that tungsten-oxide-promoted alumina–zirconia is the most active catalyst for oxidative decomposition of chloropentafluroethane (CFC-115). Hua and Sommer [54] observed that platinum-promoted $WO_3/Al_2O_3–ZrO_2$ catalyst is more active than $Pt/WO_3/ZrO_2$ for *n*-heptane isomerization in the presence of H_2 at 200 °C. Generally, it is difficult to carry out the *n*-heptane isomerization, because the cracking reaction takes place through β scission of C_7 carbenium ion intermediate [54]. As the chain length increases, such a cracking reaction is more significant than the isomerization reaction on the acid sites. It was found that molybdenum-oxide-promoted zirconia catalysts, calcined at 600–800 °C, also show strong solid acidity and

good activity for various reactions in both liquid and vapor phases [21–23]. In Mo/ZrO$_2$ catalysts, zirconia can exist in metastable tetragonal modification and this can also lead to the formation of Mo–O–Zr bonds. As the molybdenum oxide loading increases to above monolayer level or the calcination temperature is more than 650 °C, the Mo–O–Zr surface species develops into a definite Zr(MoO$_4$)$_2$ compound [34,35]. A similar analogy can be extended to Mo/Al$_2$O$_3$–ZrO$_2$ samples. These catalysts were also found to exhibit strong solid acidity and excellent catalytic activity for acid-catalyzed reactions in line with W/Al$_2$O$_3$–ZrO$_2$ [55,56]. In view of structural similarities, all these materials exhibit strong acidity and find numerous catalytic applications.

4. Conclusions

The following conclusions can be drawn from this study:

(1) The alumina–zirconia mixed oxide when calcined at 650 °C is in amorphous or poorly crystalline state. Only broad diffraction lines due to tetragonal zirconia were observed. No independent lines due to crystalline alumina are noted indicating that alumina is homogeneously mixed with the zirconia probably by forming solid solutions. On increase of calcination temperature from 650 to 750 °C, a better crystallization of zirconia tetragonal phase is observed. In particular, the incorporation of alumina into zirconia stabilizes the tetragonal phase of zirconia.

(2) The impregnation of sulfate, molybdate and tungstate promoters show a strong influence on the physicochemical properties of the Al$_2$O$_3$–ZrO$_2$ mixed oxides.

(3) The TGA–DTA results revealed that there are at least two types of sulfate species with different thermal stabilities in the case of SO$_4{}^{2-}$/Al$_2$O$_3$–ZrO$_2$ sample.

(4) The SO$_4{}^{2-}$/Al$_2$O$_3$–ZrO$_2$ sample exhibits an ammonia desorption peak maximum at 600 °C indicating superacidic nature of the catalyst.

(5) The XPS peak intensities of O 1s, Zr 3d and Al 2p and the corresponding binding energies indicate that the sulfate ion strongly interacts with the Al$_2$O$_3$–ZrO$_2$ binary oxide.

(6) Among the investigated catalysts, the SO$_4{}^{2-}$/Al$_2$O$_3$–ZrO$_2$ exhibited better product yields for acylation of alcohols and amines with acetic anhydride in the liquid phase.

Acknowledgment

References

[1] G.A. Olah, G.K.S. Prakash, J. Sommer, Superacids, Wiley, New York, 1985.
[2] K. Arata, Adv. Catal. 37 (1990) 165.
[3] A. Corma, Chem. Rev. 95 (1995) 599.
[4] K. Arata, Appl. Catal. A: Gen. 146 (1996) 3.
[5] Y. Ono, Catal. Today 81 (2003) 3.
[6] M. Hino, K. Arata, Chem. Lett. (1979) 477.
[7] X. Song, A. Sayuri, Catal. Rev.-Sci. Eng. 38 (1996) 329.
[8] G.D. Yadav, J.J. Nair, Microporous Mesoporous Mater. 33 (1999) 1.
[9] B.M. Reddy, P.M. Sreekanth, Tetrahedron Lett. 44 (2003) 4447.
[10] C.Y. Hsu, C.R. Heimbuch, C.T. Armes, B.C. Gates, J. Chem. Soc., Chem. Commun. (1992) 1645.
[11] W. Hua, A. Goeppert, J. Sommer, J. Catal. 197 (2001) 406.
[12] D.J. Rosenberg, F. Coloma, J.A. Anderson, J. Catal. 210 (2002) 218.
[13] Y. Xia, W. Hua, Z. Gao, Appl. Catal. A: Gen. 185 (1999) 293.
[14] B.M. Reddy, P.M. Sreekanth, Y. Yamada, Q. Xu, T. Kobayashi, Appl. Catal. A: Gen. 228 (2002) 269.
[15] Z. Gao, Y. Xia, W. Hua, C. Miao, Top. Catal. 6 (1998) 101.
[16] W. Hua, J. Sommer, Appl. Catal. A: Gen. 227 (2002) 279.
[17] P.J. Skrdla, C. Lindemann, Appl. Catal. A: Gen. 146 (2003) 227.
[18] S. Furuta, Appl. Catal. A: Gen. 251 (2003) 285.
[19] M. Hino, K. Arata, J. Chem. Soc., Chem. Commun. (1988) 1259.
[20] M. Scheithauer, R.K. Grasselli, H. Knözinger, Langmuir 14 (1998) 3019.
[21] B. Manohar, V.R. Reddy, B.M. Reddy, Synth. Commun. 28 (1998) 3183.
[22] B.M. Reddy, V.R. Reddy, Synth. Commun. 29 (1999) 2789.
[23] B.M. Reddy, V.R. Reddy, B. Manohar, Synth. Commun. 29 (1999) 1235.
[24] B.M. Reddy, V.R. Reddy, J. Mater. Sci. Lett. 19 (2000) 763.
[25] C.D. Wagner, W.M. Riggs, L.E. Davis, J.F. Moulder, in: G.E. Muilenberg (Ed.), Handbook of X-Ray Photoelectron Spectroscopy, Perkin-Elmer Corporation, Minnesota, 1978.
[26] , 2nd ed.D. Briggs, M.P. Seah (Eds.), Practical Surface Analysis, Auger and X-Ray Photoelectron Spectroscopy, vol. 1, Wiley, New York, 1990.
[27] W. Hua, Y. Xia, Y. Yue, Z. Gao, J. Catal. 196 (2000) 104.
[28] M.L. Guzman-Castillo, X. Bokhimi, A. Toledo-Antonio, J. Salmones-Blásquez, F. Hernandez-Beltran, J. Phys. Chem. 105 (2001) 2099.
[29] T. Klimova, M.L. Rojas, P. Castillo, R. Cuevas, J. Ramirez, Microporous Mesoporous Mater. 20 (1998) 293.
[30] D.J. Zalewski, S. Alerasool, P.K. Doolin, Catal. Today 53 (1999) 419.
[31] A. Corma, V. Fornes, M.I. Juan-Rajadell, J.M. Lopez Nieto, Appl. Catal. 116 (1994) 151.
[32] N.K. Nag, J. Phys. Chem. 91 (1987) 2324.
[33] B. Zhao, X. Wang, H. Ma, Y. Tang, J. Mol. Catal. A: Chem. 108 (1996) 167.
[34] B.M. Reddy, B. Chowdhury, E.P. Reddy, A. Fernández, J. Mol. Catal. A: Chem. 162 (2000) 431.
[35] B.M. Reddy, B. Chowdhury, P.G. Smirniotis, Appl. Catal. A: Gen. 211 (2001) 19.
[36] E. Vedejs, S.T. Diver, J. Am. Chem. Soc. 115 (1993) 3358.
[37] E.F.V. Scriven, Chem. Soc. Rev. 12 (1983) 129.
[38] A.K. Chakraborti, R. Gulhane, Tetrahydron Lett. 44 (2003) 6749.
[39] S. Chandrasekahar, T. Ramachander, M. Takhi, Tetrahedron Lett. 39 (1998) 3263.
[40] R. Kumareswaran, K. Pachamuthu, Y.D. Vankar, Synlett 11 (2000) 1652.
[41] A.G.M. Barrett, D.C. Braddock, Chem. Commun. (1997) 351.
[42] P. Kumar, R.K. Pande, M.S. Bodas, S.P. Dagade, M.K. Dongare, A.V. Ramaswamy, J. Mol. Catal. A: Chem. 181 (2002) 207.

[43] S.G. Lee, J.H. Park, J. Mol. Catal. A: Chem. 194 (2003) 49.
[44] J.M. Dominguez, J.L. Hernandez, G. Sandoval, Appl. Catal. A: Gen. 197 (2000) 119.
[45] K. Tanabe, in: M. Boudart, J.R. Anderson (Eds.), Catalysis Science and Technology, Springer-Verlag, Berlin, 1983.
[46] C.D. Baertsch, S.L. Soled, E. Iglesia, J. Phys. Chem. B. 105 (2001) 1320.
[47] K. Arata, M. Hino, Chem. Lett. (1989) 971.
[48] B.M. Reddy, V.R. Reddy, D. Giridhar, Synth. Commun. 31 (2001) 1819.
[49] B.M. Reddy, P.M. Sreekanth, Synth. Commun. 32 (2002) 2815.

[50] D.G. Barton, S.L. Soled, E. Iglesia, Top. Catal. 6 (1998) 87.
[51] S. Kuba, P. Lukinskas, R.K. Grasselli, B.C. Gates, H. Knözinger, J. Catal. 216 (2003) 353.
[52] P. Lukinskas, S. Kuba, B. Spliethoff, R.K. Grasselli, B. Tesche, H. Knözinger, Top. Catal. 23 (2003) 163.
[53] H. Nagata, S. Tashiro, M. Kishida, K. Mizuno, K. Wakabayashi, Appl. Surf. Sci. 121/122 (1997) 404.
[54] W. Hua, J. Sommer, Appl. Catal. A: Gen. 232 (2002) 129.
[55] A. Miyaji, T. Okuhara, Catal. Today 81 (2003) 43.
[56] B.M. Reddy, P.M. Sreekanth, A. Khan, Synth. Commun. 34 (2004) 1839.